¹ Manuscript submitted to **Biophysical** *Journal*

. Article

3 Push-pull mechanics of E-cadherin ectodomains in **biomimetic adhesions**

- ⁵ Kartikeya Nagendra^{1, 2}, Adrien Izzet¹, Ruben Zakine¹, Leah Friedman^{1,3}, Oliver J Harrison⁴, Léa-Laetitia Pontani⁵,
- 6 Lawrence Shapiro^{4, 6}, Barry Honig^{4, 6, 7, 8}, and Jasna Brujic^{1, 9*}
- ⁷ Center for Soft Matter Research, New York University, New York, NY 10003
- ⁸ ²Molecular Biophysics and Biochemistry Training Program, NYU Grossman School of Medicine, New York, NY 10016
- ³Département de Physique, École Normale Supérieure, PSL University, 75005 Paris, France
- ⁴Department of Biochemistry and Molecular Biophysics, Columbia University, New York, NY 10032, USA
- ⁵Laboratoire Jean Perrin, Institut de Biologie Paris-Seine, Sorbonne Université, CNRS, F-75005 Paris, France
- ⁶Zuckerman Mind Brain Behavior Institute, Columbia University, New York, NY 10027, USA
- ⁷Department of Medicine, Division of Nephrology, Columbia University, New York, NY 10032, USA
- ⁸Department of Systems Biology, Columbia University, New York, NY 10032, USA
- ⁹Laboratoire de Physique et Mécanique de Milieux Hétérogènes, UMR 7636, CNRS, ESPCI Paris-PSL, Sorbonne
- 16 Université, Université Paris Cité, 75005 Paris, France
- Correspondence: jb2929@nyu.edu

18 ABSTRACT E-cadherin plays a central role in cell-cell adhesion. The ectodomains of wild type cadherins form a crystalline- $_{19}$ like two dimensional lattice in cell-cell interfaces mediated by both trans (apposed cell) and cis (same cell) interactions. In $_{20}$ addition to these extracellular forces, adhesive strength is further regulated by cytosolic phenomena involving lpha and eta– 21 catenin-mediated interactions between cadherin and the actin cytoskeleton. Cell-cell adhesion can be further strengthened 22 under tension through mechanisms that have not been definitively characterized in molecular detail. Here we quantitatively 23 determine the role of the cadherin ectodomain in mechanosensing. To this end, we devise an E-cadherin-coated emulsion 24 system, in which droplet surface tension is balanced by protein binding strength to give rise to stable areas of adhesion. To 25 reach the honeycomb/cohesive limit, an initial emulsion compression by centrifugation facilitates E-cadherin trans-binding, hile a high protein surface concentration enables the cis-enhanced stabilization of the interface. We observe an abrupt 27 concentration dependence on recruitment into adhesions of constant crystalline density, reminiscent of a first-order phase ansition. Removing the lateral cis-interaction with a "cis mutant" shifts this transition to higher surface densities leading denser, yet weaker adhesions. In both proteins, the stabilization of progressively larger areas of deformation can be rationalized by a stiffening catch-bond, whose strength increases with tension. This catch bond may well correspond to one that has been identified in the cadherin "X-dimer".

SIGNIFICANCE The cytoskeletal role in reinforcing cell-cell adhesion is well known, but the contribution of the extracellular E-cadherin domains remains elusive. This work uses a biomimetic emulsion system to demonstrate the important 'catch-bond' behavior of E-cadherin ectodomains in response to push-pull mechanics. We find that the binding strength of E-cadherin adhesion increases with tension in both the WT and the cis-deficient MT proteins. 36 Moreover, we observe abrupt recruitment into crystalline adhesions as a function of surface concentration, consistent 37 with the proposal of a first-order phase transition at adhesion junctions. Our system is compatible with biological cells, opening the field to biophysical studies of the hybrid system.

39 INTRODUCTION

40 E-cadherin adhesion plays a crucial role in mechanical pro-41 cesses in biology, such as morphogenesis, development (1–3), maintenance of tissue structure (4–7) and tumor metastasis 43 (8, 9). *In-vivo*, cadherins form cell-cell junctions through the 44 cooperative action of trans and cis binding (10, 11). Extra-

45 cellular trans dimers undergo a homophilic interaction with a 46 free energy of binding that has been measured in vitro to be ₄₇ in the range of $9 - 10k_BT$ (12) in 3-D bulk solution. These 48 dimers laterally cluster via cis interactions on the cell surface 49 into a 2D lattice at adhesion sites, with a 2D binding energy 50 predicted to be on the order of 4 k_BT by numerical simula51 tions (13). The clustering of cadherins at adherens junctions 106 areas can be stabilized by a constant cadherin density, which

54 active mechanical sensors (17–23). More specifically, intra- 109 energy progressively increases with droplet strain, offering a ₅₅ cellular domains interact with the actin cytoskeleton through ₁₁₀ scale of binding energies from 1.6 k_BT in the weak-binding ₅₆ adaptor proteins, α and β catenin, which have been shown to 111 regime, up to 20 k_BT per molecule at the cohesive limit. Our ₅₇ be tension-dependent (24–26). Whether the mechanosensitive ₁₁₂ results suggest an intrinsic bond strengthening due to applied 58 behavior of E-cadherin is due to its intrinsic molecular prop- 113 tension, suggesting that E-cadherin mechanosensitivity is due 59 erties or due to those of the cadherin cytoskeletal complex is 114 in part to intrinsic molecular properties of E-cadherin. unclear. Of note, extracellular cadherin domains have been shown to exhibit mechanosensitive catch-bond properties in 62 single-molecule force-spectroscopy experiments (27–29).

Simplified systems of cadherin-functionalized emulsions, 116 Emulsion Preparation 64 liposomes, and model membranes, have served as useful 65 probes of the mechanisms underlying cis and trans coopera-66 tivity (30–35). Nevertheless, the mechanosensing effects of extracellular cadherin adhesion and the relative contribution 68 of cis and trans binding have not been quantified. Here, we 69 investigate extracellular cadherin adhesion in a tissue-mimetic ₇₀ emulsion, where compression and relaxation, protein surface concentration, and the presence of *cis* interactions can be 72 independently controlled.

Using emulsions, we mimic this cellular adherens junc-74 tion formation by pushing the emulsions together through calibrated pressure in the kPa range to facilitate protein 76 recruitment and adhesion (36). This applied pressure mim-77 ics the protrusive pushing forces driven by the actin-based 78 Arp2/3 complex, which are known to be necessary for cells 79 to efficiently form and extend cadherin adhesions (37). After 80 compression by centrifugation, the emulsion is allowed to 81 relax back to mechanical equilibrium, in which there is a 82 balance between surface tension and the adhesive energy of protein binding. This step aims to mimic the stabilization 84 of adhesion by cellular pulling forces (38). The resulting 85 droplet deformation allows us to estimate the average binding energy per cadherin dimer. Comparing wild type (WT) and 87 cis-deficient mutant (MT) shows that cis interactions signifi-88 cantly contribute to the stabilization of adhesions and lead to 89 larger areas of deformation (10).

91 sion response. The larger the applied pressure and therefore 92 droplet strain, the larger the equilibrium adhesion size. At 93 the maximum pressure, we reach the honeycomb limit and study the effect of cadherin surface concentration. The WT 95 self-assembles into adhesions with a constant density of ₉₆ 15.7×10^3 cadherins/µm² independent of initial concentrapropose that cis interactions drive crystallization in cadherin 99 adhesion in 2-D (13, 39). The absence of cis interactions allows the MT to freely rearrange until it reaches a jamming density of 20.1×10^3 cadherins/ μ m², which is higher than that of the WT crystal. The solid nature of these adhesions in 151 We experimentally measured the density of cadherins on the both WT and MT is confirmed by fluorescence recovery after photobleaching (FRAP) measurements. 104

driven by both intra- and extracellular interactions (14–16). 107 we interpret via a tension-dependent binding free energy of There is increasing evidence that cadherin adhesions are 108 cadherin dimers. Our experiments indicate that the binding

115 MATERIALS AND METHODS

117 The protocol for the emulsion preparation is described in (30). Briefly, the oil droplets are co-stabilized with SDS (1 mM) and the following mixtures of lipids: EPC (egg phosphatidyl-120 choline) and DGS-NTA (Ni) lipids at a molar ratio of 92:8. 121 The lipids were purchased from Avanti Polar Lipids (St. Louis, 122 MO). They were mixed to reach a total mass of about 14 mg and dried under nitrogen before the addition of 10 mL 50-cSt silicone oil purchased from Sigma Aldrich (St. Louis, MO). 125 The lipid-containing oil was then sonicated for 30 min at room temperature and heated for 3 hours at 50°C. We thus obtained an oil saturated with phospholipids. The lipid-containing oil 128 (10 mL) was then emulsified through a microfluidic chip. The 129 resulting emulsion was mono-disperse with a diameter of 130 about 20 μm. Brownian emulsion droplets were produced through membrane emulsification by a 0.5 μ m pore mem-132 brane (SPG Technology, Miyazaki, Japan), with 10 mM SDS as the continuous phase, which resulted in droplets with a diameter of approximate $4-5 \mu m$. To functionalize these droplets with DGS-NTA(Ni), 0.5 mg of DGS-NTA(Ni) was 136 dried and rehydrated with binding buffer and droplets at a 137 1: 1 ratio. The droplets were incubated with the phospholipid and binding buffer mix overnight at room temperature and 139 gentle rotation.

140 Cadherin Grafting

For both WT and MT, we find a pressure-sensitive adhe- 141 Binding buffer was prepared containing 3.8mM calcium, 2 142 mM EDTA, 20 mM Tris, 10 mM NaCl, 10 mM KCl, pH = 7, and 1 mM SDS in a 50:50 glycerol/water solution for refractive 144 index matching. The emulsion was mixed with binding buffer 145 at 40% volume fraction and then incubated with varying con-146 centrations of His-tagged E-cadherin ectodomains in 50 μ L 147 of binding buffer containing EDTA. Low concentrations of tion. This finding is consistent with numerical simulations that 148 salts were added to reduce nonspecific adhesions between the 149 droplets.

150 Cadherin Density Estimation

droplet surface at droplet saturation. The fluorescence intensity of a solution of 1 μ M WT E-cadherin, containing 3.0×10^{13} Interestingly, we observe that a wide range of adhesion 154 molecules was measured through a fluorimeter (Horiba-PTI 155 QM-400 Fluorescent spectrometer). Upon adding droplets at 204 **RESULTS** 40% volume fraction and 1.8 mM calcium, we observed a 62%This loss of intensity from the bulk solution indicated that approximately 1.8×10^{13} cadherin molecules migrated from the bulk solution on to the droplets. We estimated the droplet density to be about $3.2 \times 10^4 / \mu l$, corresponding to a total droplet count of about 1.6×10^6 in a 50μ l sample. Therefore, there were approximately 1.2×10^7 cadherin molecules per droplet. For a droplet of radius 10 μ m, the surface area is $1256 \,\mu\text{m}^2$. The density of cadherins at saturation is approximately $9.3 \times 10^3 / \mu m^2$. Therefore, a saturation intensity of 150 A.U. for WT cadherin and 120 A.U. for MT cadherin corresponded to a cadherin surface density of $9.3 \times 10^4 / \mu m^2$. The fluorescence measurements are shown in Fig. S1.

Confocal Microscopy

171 The droplets were grafted with cadherin proteins which were fluorescently labeled with Alexa 488. The buffer was refractive index matched with glycerol for transparency, which allowed for imaging of the emulsion in 3-D. We used a fast-scanning confocal microscope (TCS SP5 II; Leica Microsystems, Buf-176 falo Grove, IL)

177 Centrifugation and Pressure Measurement

178 The experimental setup involved cadherin-functionalized droplets contained in a capillary, 5mm and 100μ m in depth (VitroTubes, NJ). The droplets in the capillary were compressed in a centrifuge at speeds ranging from 50g up to 800g, after which they were allowed to relax over a 48-hour period. 231 where $\rho_{\rm max}$ is the cadherin saturation density and K_{eq} is the The pressure inside the compressed aggregate was estimated through the relation $P = \Delta \rho g h$, where P is the hydrostatic pressure, $\Delta \rho$ is the density difference between silicon oil and water, and h is the height of the compressed aggregate pile which was measured after centrifugation and equilibration of 188 droplets.

189 Fluorescence Recovery after Photobleaching

191 Droplets functionalized with cadherin were placed in a glass 242 consequence of the entropy loss upon calcium stiffening of the 193 at 800g to form a cohesive 3-D droplet aggregate, which 244 does not affect the surface tension because the proteins are not adhesions and free perimeters were identified and marked as 246 lipids (44). regions of interest. A laser pulse of ~ 200mW was applied 247 model $I = I_{\text{max}}(1 - e^{-t/\tau})$, where I is the normalized intensity, 252 calcium without cadherins, as shown in Fig. S3. However, they I_{max} is the pre-photobleach intensity, t is time, and τ is the 253 do bind to form diffusion-limited aggregates (DLA) (46) in the 203 characteristic recovery time.

205 Our biomimetic emulsion system mimics the outer cell memloss in fluorescence intensity of the 1 μ M cadherin solution. ₂₀₆ brane, but replaces the cytoskeleton with silicone oil, as shown 207 in Fig. 1A. The oil-in-water interface has a surface tension of ²⁰⁸ 7mN/m in Fig. S2 A and B. The monolayer membrane is stabi-209 lized by a mixture of SDS, Egg-PC (EPC), and DGS-NTA-Ni 210 phospholipids, which serve to functionalize the droplets with 211 E-cadherin (30, 41). Droplets are generated using microflu-212 idics, which gives rise to monodisperse ($D = 20 \pm 1 \,\mu\text{m}$) emulsions that are stable against coalescence. This synthesis 214 allows for their compression into a biliquid foam structure 215 resembling cohesive tissues, as shown in Fig. 1 B, C.

> These emulsions are visualized under a confocal mi-217 croscope, revealing uniform cadherin fluorescence on the 218 surface of the droplets, as shown in the inset in Fig. 2A. 219 Cadherins depend on calcium ions for their adhesive function (42). Specifically, the ectodomains are comprised of tandem immunoglobulin-like domains that bind calcium, which 222 increases their rigidity to form a crescent shape (43). This 223 conformation enables them to bind other cadherins through 224 trans interactions across cells and cis interactions on the 225 same cell. Histograms of fluorescence intensity on the droplet surface reveal that adding calcium $[Ca^{2+}]$ increases cadherin surface adsorption. Converting the intensity to protein density ρ (see Methods) allows us to quantify the surface adsorption 229 of bulk cadherin [cad], as shown in Fig. 2B. Both WT and 230 MT data are well fit with the Langmuir adsorption isotherm

$$\frac{\rho}{\rho_{\text{max}}} = \frac{[\text{cad}]K_{eq}}{1 + [\text{cad}]K_{eq}},\tag{1}$$

232 equilibrium constant for the His-tag-nickel interaction, whose value in the presence of calcium was estimated to be 4×10^{-12} . Note that in the presence of calcium, cadherin preferentially partitions into the aqueous phase above [cad] = 1 μ M, likely 236 due to protein aggregation. We find that adding physiological 1.8mM for [Ca²⁺] increases $\rho_{\rm max}$ by 25%, which corresponds 238 to a decrease in inter-cadherin distance from 9.1 to 8.1 nm, 239 almost reaching the crystalline packing limit at 7.2 nm (10). The ratio of K_{eq} with and without calcium yields a free energy difference of 0.3 k_BT. This adsorption enhancement may be a capillary. The droplet-containing capillaries were centrifuged 243 proteins, as illustrated in Fig. 2C. The protein concentration was then visualized through confocal microscopy. Suitable 245 adsorbed at the interface, but are carried by the functionalized

Having characterized the density of proteins on the surface, for 1.5 minutes to the FRAP region of interest in order to 248 we demonstrate their adhesive function via an aggregation photobleach. FRAP intensity trajectories were fit using custom 249 assay (45). Thermal emulsion droplets of diameter 5 μ m, MATLAB code that subtracted background, normalized the 250 functionalized with either WT or MT, do not adhere in the intensities to their pre-bleach level, and fit to an exponential 251 absence of calcium, nor do they adhere in the presence of 254 presence of proteins and calcium, as shown in Fig. 2D. These

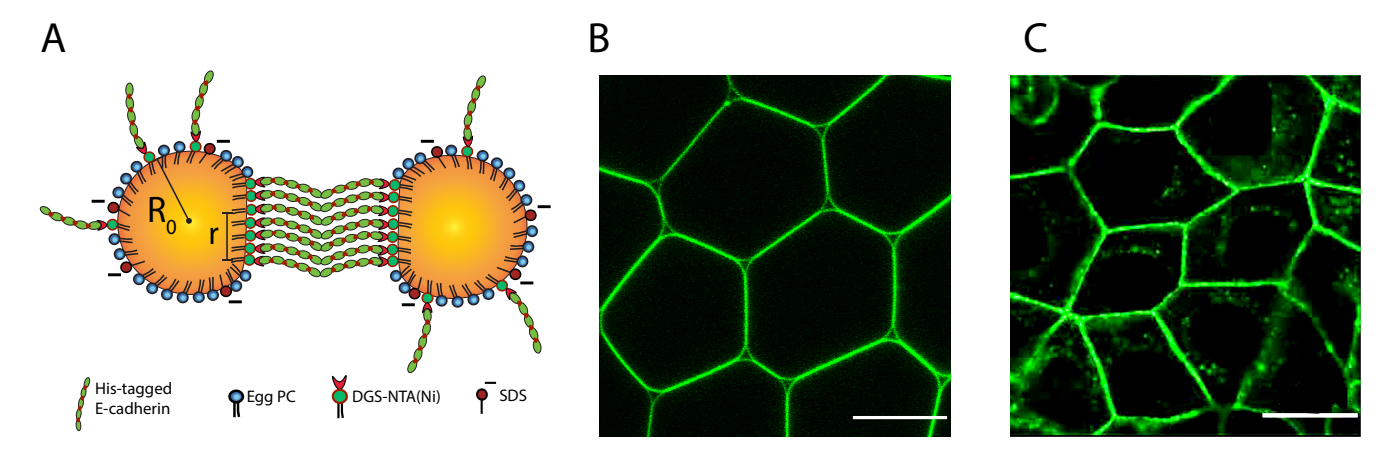


Figure 1: (A) Schematic representation of biomimetic emulsion droplets. Droplets consist of silicon stabilized through phospholipids and SDS. Lipids with a NTA(Ni) group allow for the binding of His-tagged cadherin ectodomains. (B) Biomimetic emulsion droplets functionalized with fluorescent E-cadherin extracellular domain form a confluent tissue-like structure. (C) Cadherin-expressing living cells form a confluent packing through cadherin binding (40). Scale bar: $20\mu m$.

₂₅₅ branched structures have on average three droplet neighbors in WT or MT adhesion, consistent with DLA theory, as shown in Fig. 2E. 257

Using large cadherin-coated droplets the size of biolog-258 259 ical cells, we study the effects of concentration and applied 260 pressure on cadherin-cadherin adhesion strength in both WT and MT proteins. Gravity alone is insufficient to deform the 261 droplets away from spherical because the kinetic barrier to adhesion is too high. Instead, applying a centrifugation rate of 800g, corresponding to a compression of 4.8 kPa, deforms the droplets into a foam and facilitates cadherin recruitment 266 into adhesions. We subsequently allow the system to relax for 48h to reach mechanical equilibrium where the surface 267 tension force is balanced by the cadherin binding forces, as shown in Figs. 3A, B. Droplet relax back to spheres in the 269 absence of calcium within 15 minutes, Fig. S4.

Control experiments show that cadherin adhesion is only activated in the presence of calcium, otherwise the droplets lizes progressively larger adhesions in both the WT and MT 276 proteins, as shown in Fig. 4A. For each concentration, the adhesive emulsions are refractive index matched for visualization 278 in 3-D (47), as shown in Fig. 4B, C. Image analysis identifies 279 the average intensity and the adhesion area A, which in turn give the density and a corresponding number of cadherins Nin each adhesion patch. Here N is measured directly from the cadherin fluorescence intensity, and converted to density after mechanical equilibrium is reached. The broad distribution of patch radii arises from the heterogeneous droplet packing geometry and stresses therein (47). Figure 4D shows that the WT on average stabilizes larger patches than the MT under 287 the same experimental conditions.

 E_d stored in a system consisting of two droplets in contact. In the limit of small deformations and given a constant surface tension $\gamma = 7 \pm 0.5$ mN/m across the droplet interface (48), we have

$$E_d = \frac{2\gamma}{S_0} A^2,\tag{2}$$

where $S_0 = 4\pi R_0^2$ denotes the area of the spherical droplet of radius R_0 and A is the contact area of adhesion. In mechanical equilibrium, this energy of deformation is balanced by the total free energy of binding $N \times e_b$ of N cadherin molecules. Using (2), the binding energy per cadherin bond e_b is thus given by

$$e_b = \frac{2\gamma A^2}{S_0 N}. (3)$$

This result predicts $A = \left(\frac{e_b S_0}{2\gamma}\right)^{1/2} N^{1/2}$ or equivalently $A = \int_0^{2\pi} dt dt$ return to their spherical shape. With calcium, increasing the return to their spherical shape. With calcium, increasing the return to their spherical shape. With calcium, increasing the return to their spherical shape. With calcium, increasing the return to their spherical shape. With calcium, increasing the return to their spherical shape. With calcium, increasing the return to their spherical shape. With calcium, increasing the return to their spherical shape. With calcium, increasing the return to their spherical shape. With calcium, increasing the return to their spherical shape. With calcium, increasing the return to their spherical shape. With calcium, increasing the return to their spherical shape. With calcium, increasing the return to their spherical shape. low initial concentrations ρ_i (under 4.8 kPa compression) and 292 gives $e_b = 1.6 \pm 0.3 \text{ k}_B\text{T}$ in the case of the MT. This free 293 energy of trans binding alone is in the range predicted by 294 computational studies that take into account the rotational and ²⁹⁵ vibrational entropy loss upon confinement and dimerization 296 in 2D (49).

Above a threshold ρ , the cadherins jam into patches of a constant density $(A \propto N) \rho_{\rm MT} = 20.1 \times 10^3 / \mu \rm m^2$. Increasing ρ_i enhances the probability to make larger adhesion patches, 300 but does not change their density. This MT density corresponds 301 to an average inter-cadherin distance of 6.9 ± 0.1 nm, which 302 agrees with the jamming limit of the random packing of disks 303 (50). On the other hand, WT adhesions are comprised of From these data, we estimate the free energy of binding per both cis and trans-interacting cadherins, which forces them molecule e_b . First, we estimate the total deformation energy 305 to crystallize at a lower density of $\rho_{\rm WT} = 15.7 \times 10^3 / \mu {\rm m}^2$,

271

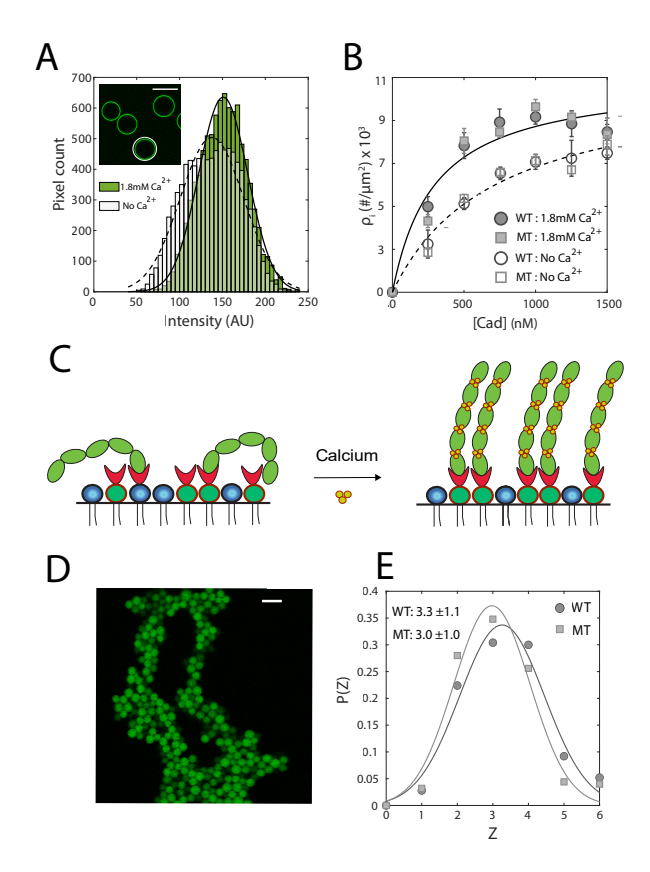


Figure 2: (A) Distribution of pixel brightness for a given droplet, measured on the focal plane that displays the larger ring diameter. The average intensity in presence of calcium (green histogram) is larger that the average intensity without (white histogram), indicating that calcium favors the recruitment of cadherins at the droplet surface. (B) Cadherin surface adsorption density ρ_i as a function of cadherin bulk concentration [Cad]. Adsorption at the droplet surface increases when bulk density increases, and saturates when [Cad] $\simeq 10^3$ nM. Addition of calcium in the medium yields a higher cadherin surface density up to $\rho_i \simeq 9.3 \times 10^3 \, \mathrm{cad/\mu m^2}$. (C) Schematic representation of calcium binding to cadherins. Calcium binding rigidifies cadherins, giving them a crescent shape, which is crucial to forming trans dimers. Rigidified cadherins also leave more surface area open for the binding of additional cadherins to the droplet. (D) Cadherin-coated Brownian droplets (green disks) form large aggregates upon calcium addition, confirming homophilic adhesion. Scale bar: 20 µm.(E) Distribution of coordination number for WT and MT cadherin-coated droplets. Both WT and MT form droplet aggregates of mean coordination number $\langle Z \rangle = 3$.

308 distance of 7.9 nm, which is in good agreement with the 322 same linear increase of A vs. N, i.e., constant cadherin packing ³⁰⁹ reported crystal lattice distances of 7.2 to 7.9 nm, as measured ³²³ density, for the WT and MT as those observed in Fig. 5A,

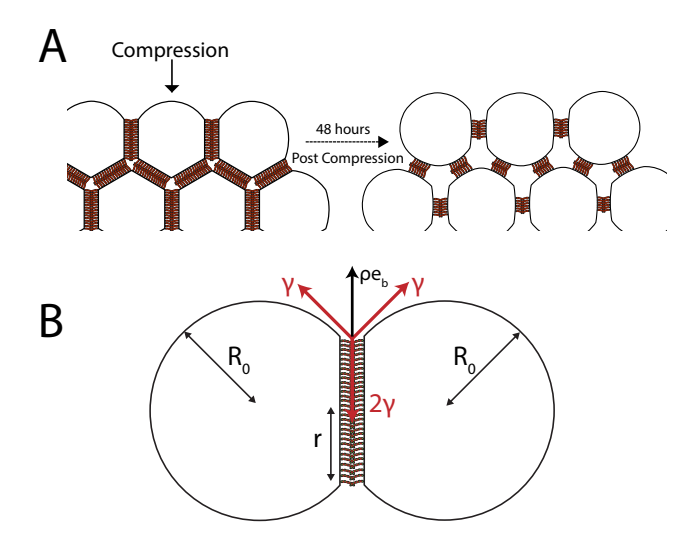


Figure 3: (A) Droplets adopt a foam-like structure through centrifugation. Over 48 hours, the system relaxes to a foam under tension, where cohesion is maintained by the cadherinpopulated patches between neighbouring droplets. Compressed droplets attempt to relax back to spheres under the influence of droplet surface tension and the re-entry of aqueous buffer. (B) Expanded view of the force balance between two adhesive droplets of uncompressed radii R_0 and adhesion radius r, with cadherin density ρ . Mechanical equilibrium is maintained in adhesive droplets through the balance between cadherin binding energy e_b and droplet surface tension γ .

310 by crystallography or electron microscopy of liposome and 311 cell-cell adhesions (10, 51).

Assuming a constant e_b per molecule in (3), a given cadherin density fixes the area of deformation. However, our data shows that patches of the same density give rise to increasing adhesion sizes as a function of the applied pressure. We therefore interpret our experimental results in terms of the e_b increase with droplet deformation, quantified as the area strain of a droplet,

$$\xi = \frac{S - S_0}{S_0},\tag{4}$$

where ${\cal S}$ denotes the area of the deformed droplet and, in the limit of small deformations, $S - S_0 = \sum_{i=1}^n A_i^2 / S_0$ (52), where index i labels the patches on a droplet with n contacts. 315 In the limit of maximum compression into a biliquid foam, we measure the number of contacts per droplet n = 12 (53, 54), and we can thus set the local strain of a contact patch of 318 area A to be $\xi \simeq 12A^2/S_0^2$.

To maximize the extent of adhesion we saturate ρ_i to ₃₀₆ also shown in the figure. This patch density is independent ₃₂₀ $9.3 \times 10^3/\mu\text{m}^2$, and test the effect of the applied pressure of initial concentration. It corresponds to an inter-cadherin 321 ranging from 0.3 kPa to 4.8 kPa. In Fig. 5B, we show the

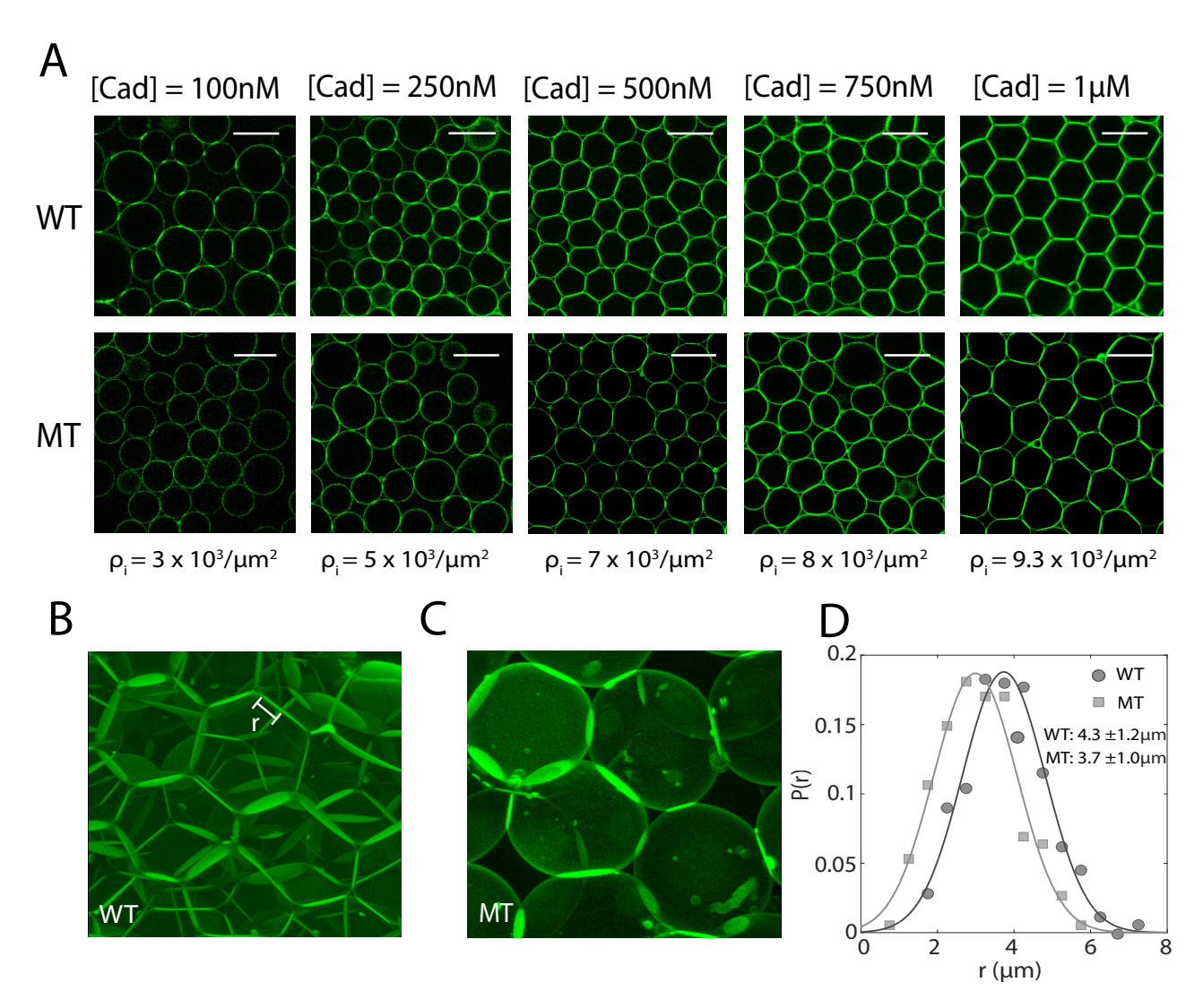


Figure 4: (A) Final configuration of the system after compression at 4.8kPa and 48h relaxation, for different concentrations of bulk cadherins, both for WT (upper panels) and MT (lower panels). Droplets of varying cadherin surface densities were centrifuged, resulting in the formation of irreversible adhesions and deformations. Scale bar: 20 µm. (B, C) 3-D reconstruction of compressed droplets for WT (panel B) and MT (panel C). Cadherins are concentrated at sites of adhesion upon compression. For each patch, the radius r is measured, and yields the patch area A. Panel width corresponds to $40\mu m$. (D) Distribution of patch radii for both WT and MT systems. For (B), (C) and (D): surface density $\rho_i = 9.3 \times 10^3 \text{cad/} \, \mu\text{m}^2$ and compression P = 4.8kPa.

³²⁴ confirming protein crystallization or jamming, respectively. ³³⁶ The amplitude of the stress response of the MT is 3/4 of ³²⁵ Increasing the pressure forms progressively larger adhesion ³³⁷ that of the WT, highlighting the importance of *cis* and *trans* areas, similar to the effect of increasing ρ_i at constant pressure 338 cooperativity in stabilizing adhesion. in Fig. 5A. Both ρ_i and the applied pressure, therefore, play 339 an important role in stabilizing adhesions. 328

Next, we plot the percentage of recruited proteins into 340 adhesions as a function of both pressure and concentration, We find $e_b \propto \xi^{1/2}$, see Fig. 5C. This result is indicative of a 341 see Fig. 5D. Since increasing pressure linearly increases the force-dependent adhesion response, where the cadherin-dimer 342 area of adhesion, it also linearly increases the fraction of bond is strengthened in response to deformation, suggesting a 343 recruited molecules, consistent with a random attachment catch-bond behavior (29). While both WT and MT show a 344 model at fixed concentration. Conversely, increasing ρ_i at 393 continuously increasing binding free energy, the WT stabilizes 345 fixed pressure, we observe a sharp non-linear increase in and larger adhesion patches than the MT and reaches higher 346 recruitment for both WT and MT above a common threshold binding energies of up to 20k_BT at the cohesive droplet limit. 347 density, see Fig. 5D. This behavior is reminiscent of a density-

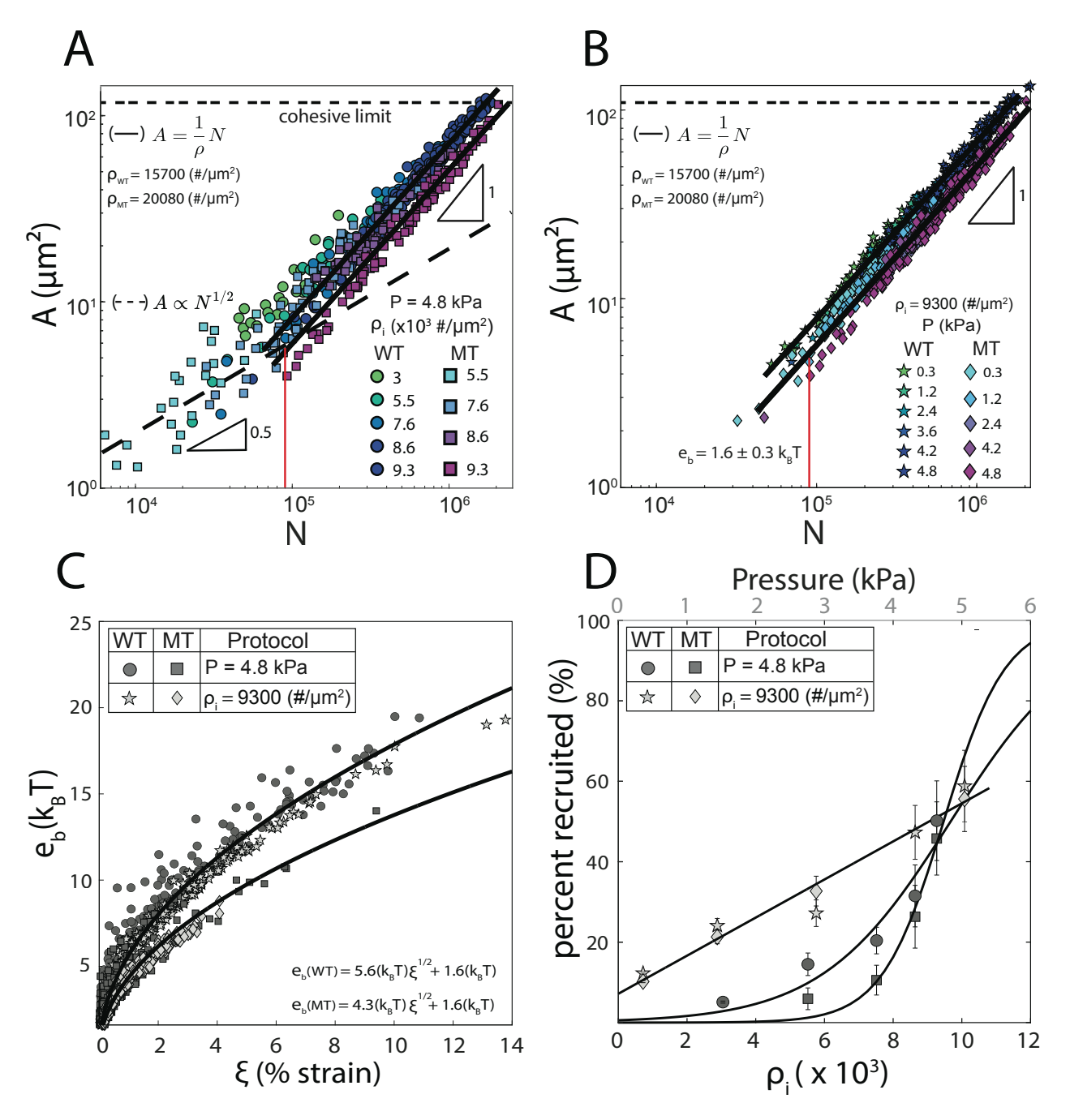


Figure 5: (A) Area A of patches as a function of cadherin number N in the patch for different cadherin surface concentration ρ_i in WT and MT systems, at a given compression P = 4.8kPa. We identify two regimes. For low cadherin number, the data follows $A \propto N^{1/2}$ (black dashed line), yielding an estimate of $e_b = 1.6 \pm 0.3 \ k_B T$. For larger N, the data follows $A \propto N$, indicating constant density in the patches. (B) Area of patches A, as a function of the number of cadherins N in the patch for fixed cadherin surface concentration ρ_i and different values of compression. The compression ranges from about 0.3 to 4.8 kPa. For both WT and MT, we observe $A \propto N$, indicating that adhesions are growing at a constant density. For the WT the density is $\rho_{\rm WT} = 15.7 \times 10^3 {\rm cad}/\mu{\rm m}^2$, while the MT adhesions are denser at about $\rho_{\rm MT} = 20.1 \times 10^3 {\rm cad}/\mu{\rm m}^2$. (C) Binding energy e_b per cadherin bond as a function of the area strain ξ of the deformed droplets, for both pressure and density evolution as shown in in panel A and B. Since $e_b = 2\gamma A^2/(NS_0)$ and $A = \rho N$ with constant density, e_b varies with deformation (D) Fraction of cadherins recruited as a function of varying cadherin density and pressure. Circles (WT) and squares (MT) show cadherin recruitment as a function of cadherin density (ρ_i) . An empirical fit demonstrates the sigmoidal nature of the recruitment with an inflection point around 9500cad/µm². Stars (WT) and diamonds (MT) show recruitment evolution as a function of applied pressure (top axis). Varying the pressure from 0.3 to 4.8 kPa leads to a linear growth in recruitment for both WT and MT.

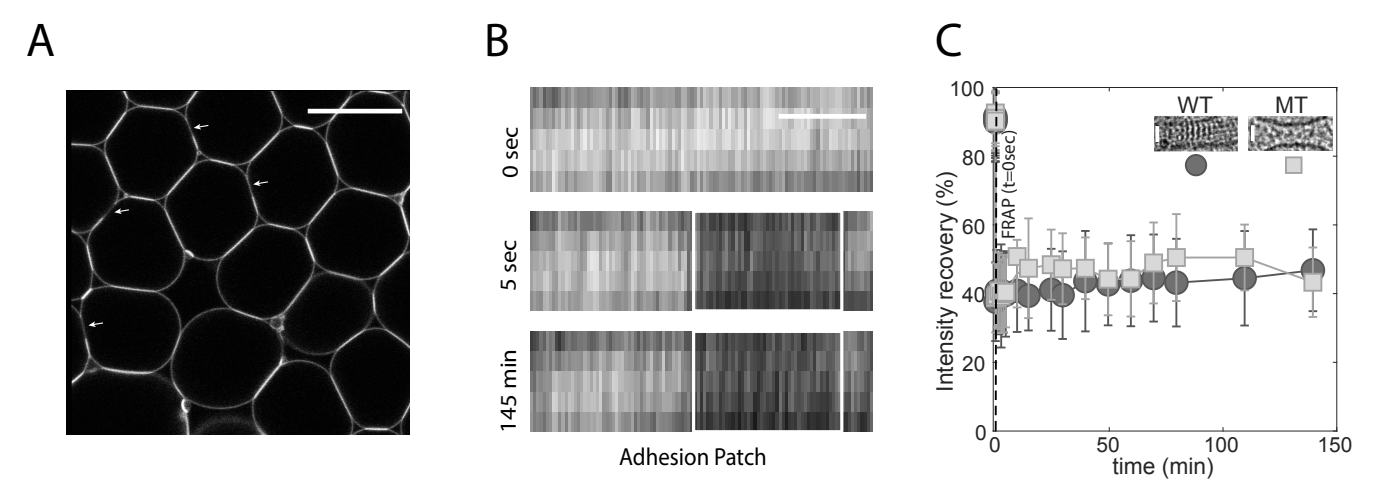


Figure 6: (A) Focus on a loosely packed region in the capillary for WT cadherin-saturated droplets ($\rho_i = 9.3 \times 10^3 \text{cad}/\mu\text{m}^2$) and maximal compression at P = 4.8kPa. Arrows indicate photobleached regions on adhesion patches. Scale bar: 20μ m. (B) Magnified view of an adhesion before and after FRAP. Scale bar: $1\mu m$. The photobleached regions of patches do not recover initial brightness, whether WT or MT, indicating a jammed state in the patches in both situations. (C) Quantitative measurement of recovery intensity after FRAP, for both WT and MT. Inset: electron-microscopy of patches made of WT or MT, reproduced from (10).

in cadherin ectodomains (13, 39).

351 352 354 at the saturation cadherin ρ_i used in these experiments.

DISCUSSION

350

368 In this paper we have established that our biomimetic emul- 400 Most notably, our experiments provide a clear demonstration faces and recapitulate its role in enabling trans dimerization. 406 between cells. Second, as observed in cells, WT cadherins coated on droplet 376 surfaces spontaneously organizes into adhesions with a crystalline density, driven by both trans and cis interactions. Third,

gas dependent phase-transition that has been predicted to occur 378 we find that the MT does not form a crystalline lattice, but, 379 rather, jams into clusters with a higher density than the WT. Our density measurements in Fig. 5 suggest that WT 380 This tendency of the MT to form dense adhesions through and MT adhesions are solid-like, either in a crystalline or a 381 non-specific lateral interactions has also been observed prerandomly jammed array. To test this hypothesis, we FRAP 382 viously in lipid bilayer systems (56). Our most important sections of many adhesion zones, as shown in Fig. 6. Both 383 finding is that both WT and MT are mechanosensitive, and protein types do not fully bleach, but preserve 40% of the initial 384 that this is a property of the ectodomain alone. It is known that fluorescence after a one minute laser pulse. We do not observe 385 cadherins are capable of mechanosensitive force-dependent any subsequent fluorescence recovery, consistent with solid 386 tuning of their adhesion by acting like catch-bonds under adhesions. However, bleaching the proteins that are outside the 387 tensile stress(27-29, 57, 58). The formation of this catch bond adhesions uncovers two cadherin populations that recover over 388 is a property of the cadherin X-dimer (59) which corresponds significantly different timescales, $\tau_1 = 44$ s and $\tau_2 = 523$ s, so to an alternate conformation to the canonical strand-swapped respectively. Their diffusion constants, given by $D = r_b^2/(4\tau)$, so cadherin dimer. A number of studies have detected X-dimers where r_b is the radius of the circular photobleached region, 391 on cell surfaces (60, 61). In addition FRET-based measureyield $D_1 = 2.2 \times 10^{-2} \ \mu\text{m}^2/\text{s}$ and $D_2 = 2.0 \times 10^{-3} \ \mu\text{m}^2/\text{s}$, so ments of cis and it trans-cooperativity have shown that bond Fig. S5. The fast recovery is consistent with the diffusion of 393 lifetimes are greatly increased due to cis interactions (32). lipids on the surface of a silicon oil emulsion (55), while the 394 Our results suggest a similar cis-contribution to the binding slow recovery may be a result of lateral crowding interactions 395 energies, where WT cadherins are able to reach higher binding ³⁹⁶ energies compared to the *cis* mutant. Here we establish that 397 catch bonds are formed as a consequence of applied pressure 398 and with increasing droplet deformation, we estimate increas-399 ing binding energy to reach 20k_BT for WT and 14k_BT for MT. sion system can recapitulate a number of known E-cadherin 401 that catch bonds can be formed under conditions that mimic dependent phenomena and thus constitutes a useful platform 402 cellular forces thus opening the door to experiments, for examto study a range of phenomena associated with cadherin- 403 ple with mutant protein aimed at directly establishing a role mediated cell-cell adhesion. First, we quantify the effect of 404 for X-dimers in the E-cadherin mechanosensitive response calcium on the packing density of cadherins at droplet inter- 405 and, more generally, in regulating the transmission of forces

407 AUTHOR CONTRIBUTIONS

408 L.S., B.H., L.L.P., and J.B. designed the study and wrote 409 the paper. K.N. designed and performed experiments, ana-454 410 lyzed experimental data and wrote the paper, A.I. analyzed 455 experimental data, R.Z. developed theory, L.F. analyzed ex-456 412 perimental data, O.J.H. expressed and purified proteins.

CKNOWLEDGMENTS

414 We thank Sergey Troyanovsky, Angus McMullen, and Sascha 415 Hilgenfeldt for helpful discussions. This work was sup-416 ported by the NIH Molecular Biophysics Training Grant 417 T32 GM088118, NSF MCB 19101542, the Paris Region (Région Île-de-France) under the Blaise Pascal International ⁴¹⁹ Chairs of Excellence, the Emergence(s) grant from the Ville de Paris, and the National Science Foundation under grants 466 ⁴²¹ No. NSF PHY17-48958 and No. NSF DMR-1710163.

COMPETING INTERESTS

423 The authors declare no competing interests

REFERENCES

439

440

442

- 1. M Takeichi. "The cadherins: cell-cell adhesion molecules 474 425 controlling animal morphogenesis". In: Development 475 426 102.4 (1988), pp. 639-655.
- 2. Jennifer M. Halbleib and W. James Nelson. "Cadherins 477 in development: cell adhesion, sorting, and tissue mor- 478 429 phogenesis". en. In: Genes & Development 20.23 (2006), 479 13. Yinghao Wu et al. "Cooperativity between trans and cis pp. 3199–3214. ISSN: 0890-9369, 1549-5477. DOI: 10. 480 431 1101/gad.1486806.
- 3. Carien M. Niessen, Deborah Leckband, and Alpha S. Yap. 482 433 "Tissue Organization by Cadherin Adhesion Molecules: 483 434 Dynamic Molecular and Cellular Mechanisms of Mor- 484 435 phogenetic Regulation". In: Physiological Reviews 91.2 485 (2011), pp. 691–731. ISSN: 0031-9333. DOI: 10.1152/ 486 437 physrev.00004.2010. 438
 - 4. Floor Twiss and Johan de Rooij. "Cadherin mechan-488 otransduction in tissue remodeling". en. In: Cellular and 489 Molecular Life Sciences 70.21 (2013), pp. 4101-4116. 490 ISSN: 1420-9071. DOI: 10.1007/S00018-013-1329-X. 491
- 5. Jean-Léon Maître and Carl-Philipp Heisenberg. "Three 492 443 444 Biology 23.14 (2013), R626–R633. ISSN: 0960-9822. DOI: 494 445 10.1016/j.cub.2013.06.019.
- 6. Marita Goodwin and Alpha S. Yap. "Classical cadherin adhesion molecules: coordinating cell adhesion, signal-448 ing and the cytoskeleton". en. In: Journal of Molecular 498 449 Histology 35.8-9 (2004), pp. 839–844. ISSN: 1567-2379, 499 450 1573-6865. DOI: 10.1007/s10735-004-1833-2.

- 7. K. Venkatesan Iyer et al. "Epithelial Viscoelasticity Is Regulated by Mechanosensitive E-cadherin Turnover". English. In: Current Biology 29.4 (2019), 578–591.e5. ISSN: 0960-9822. DOI: 10.1016/j.cub.2019.01.021.
- 8. Yuliya I. Petrova, Leslayann Schecterson, and Barry M. Gumbiner. "Roles for E-cadherin cell surface regulation in cancer". In: Molecular Biology of the Cell 27.21 (2016), pp. 3233–3244. ISSN: 1059-1524. DOI: 10.1091/mbc. E16-01-0058.

457

459

461

467

469

470

- 9. Michalina Janiszewska, Marina Candido Primi, and Tina Izard. "Cell adhesion in cancer: Beyond the migration of single cells". In: The Journal of biological chemistry 295 (8 2020), pp. 2495–2505. ISSN: 1083-351X. DOI: 10.1074/JBC.REV119.007759.
- 10. Oliver J. Harrison et al. "The Extracellular Architecture of Adherens Junctions Revealed by Crystal Structures of Type I Cadherins". en. In: Structure 19.2 (2011), pp. 244– 256. ISSN: 0969-2126. DOI: 10.1016/j.str.2010.11. 016.
- 11. Barry Honig and Lawrence Shapiro. "Adhesion protein structure, molecular affinities, and principles of cell-cell recognition". en. In: Cell 181.3 (2020), pp. 520-535.
- 12. P. Katsamba et al. "Linking molecular affinity and cellular specificity in cadherin-mediated adhesion". en. In: Proceedings of the National Academy of Sciences 106.28 (2009), pp. 11594–11599. issn: 0027-8424, 1091-6490. DOI: 10.1073/pnas.0905349106.
- interactions in cadherin-mediated junction formation". en. In: Proceedings of the National Academy of Sciences 107.41 (2010), pp. 17592–17597. issn: 0027-8424, 1091-6490. DOI: 10.1073/pnas.1011247107.
- 14. A S Yap, C M Niessen, and B M Gumbiner. "The juxtamembrane region of the cadherin cytoplasmic tail supports lateral clustering, adhesive strengthening, and interaction with p120ctn". en. In: J. Cell Biol. 141.3 (1998), pp. 779-789.
- 15. Binh-An Truong Quang et al. "Principles of E-Cadherin Supramolecular Organization In Vivo". en. In: Current Biology 23.22 (2013), pp. 2197–2207. issn: 0960-9822. DOI: 10.1016/j.cub.2013.09.015.
- Functions of Cadherins in Cell Adhesion". en. In: Current 493 16. Hong, S, Regina B. Troyanovsky, and Sergey M. Troyanovsky. "Binding to F-actin guides cadherin cluster assembly, stability, and movement". In: Journal of Cell Biology 201.1 (2013), pp. 131–143. DOI: 10.1083/jcb. 201211054.
 - 17. Zhijun Liu et al. "Mechanical tugging force regulates the size of cell-cell junctions". In: Proc. Natl. Acad. Sci. U. S. A. 107.22 (2010), pp. 9944–9949.
 - 18. Benoit Ladoux et al. "Strength dependence of cadherinmediated adhesions". In: Biophys. J. 98.4 (2010), pp. 534-502 542. 503

- 504 19. Hamid Tabdili et al. "Cadherin-dependent mechanotrans- 555 31. P.-H. Puech, H. Feracci, and F. Brochard-Wyart. "Adduction depends on ligand identity but not affinity". In: J. 556 Cell Sci. 125.Pt 18 (2012), pp. 4362–4371. 506
- 20. William A Thomas et al. " α -Catenin and vinculin cooper-507 ate to promote high E-cadherin-based adhesion strength". 508 In: J. Biol. Chem. 288.7 (2013), pp. 4957–4969.
- 21. Quint le Duc et al. "Vinculin potentiates E-cadherin 510 mechanosensing and is recruited to actin-anchored sites 511 within adherens junctions in a myosin II-dependent man-512 ner". In: J. Cell Biol. 189.7 (2010), pp. 1107–1115. 513
- 22. Adrienne K Barry et al. "A-catenin cytomechanics—role in 514 cadherin-dependent adhesion and mechanotransduction". In: J. Cell Sci. 127.Pt 8 (2014), pp. 1779–1791. 516
- 517 23. Caitlin Collins et al. "Changes in E-cadherin rigidity sensing regulate cell adhesion". In: Proceedings of the 518 National Academy of Sciences of the United States of 519 America 114.29 (2017), E5835–E5844. ISSN: 0027-8424. DOI: 10.1073/pnas.1618676114. 521
- 522 24. Shigenobu Yonemura et al. " α -Catenin as a tension transducer that induces adherens junction development". In: 523 Nature Cell Biology 2010 12:6 12 (6 2010), pp. 533–542. 524 ISSN: 1476-4679. DOI: 10.1038/ncb2055. 525
- 25. Nicolas Borghi et al. "E-cadherin is under constitutive 526 actomyosin-generated tension that is increased at cell-cell 527 contacts upon externally applied stretch". In: *Proc. Natl.* 528 Acad. Sci. U. S. A. 109.31 (2012), pp. 12568–12573.
- 530 26. Rima Seddiki et al. "Force-dependent binding of vinculin to α -catenin regulates cell-cell contact stability 531 and collective cell behavior". In: Molecular Biology 532 of the Cell 29 (4 2018), p. 380. ISSN: 19394586. DOI: 533 10.1091/MBC.E17-04-0231.
- 27. Kristine Manibog et al. "Resolving the molecular mechanism of cadherin catch bond formation". en. In: Na-536 ture Communications 5.1 (2014). ISSN: 2041-1723. DOI: 537 10.1038/ncomms4941. 538
- 539 28. Kristine Manibog et al. "Molecular determinants of cadherin ideal bond formation: Conformation-dependent unbinding on a multidimensional landscape". en. In: *Pro-*541 ceedings of the National Academy of Sciences 113.39 542 (2016), E5711–E5720. ISSN: 0027-8424, 1091-6490. DOI: 10.1073/pnas.1604012113. 544
- 545 29. Sabyasachi Rakshit et al. "Ideal, catch, and slip bonds in cadherin adhesion". en. In: Proceedings of the Na-546 tional Academy of Sciences 109.46 (2012), pp. 18815– 547 18820. ISSN: 0027-8424, 1091-6490. DOI: 10.1073/ pnas.1208349109. 549
- 550 30. Lea-Laetitia Pontani, Ivane Jorjadze, and Jasna Brujic. "Cis and Trans Cooperativity of E-Cadherin Mediates 551 Adhesion in Biomimetic Lipid Droplets". en. In: Biophys-552 ical Journal 110.2 (2016), pp. 391–399. issn: 0006-3495. DOI: 10.1016/j.bpj.2015.11.3514. 554

- hesion between Giant Vesicles and Supported Bilayers Decorated with Chelated E-Cadherin Fragments". In: Langmuir 20.22 (2004), pp. 9763–9768. ISSN: 0743-7463. DOI: 10.1021/la048682h.
- Connor J. Thompson et al. "Cadherin cis and trans interactions are mutually cooperative". en. In: Proceedings of the National Academy of Sciences 118.10 (2021), e2019845118. ISSN: 0027-8424, 1091-6490. DOI: 10. 1073/pnas.2019845118.

561

- Kabir H. Biswas et al. "E-cadherin junction formation involves an active kinetic nucleation process". en. In: Proceedings of the National Academy of Sciences 112.35 (2015), pp. 10932–10937. issn: 0027-8424, 1091-6490. DOI: 10.1073/pnas.1513775112.
- Yu Cai et al. "Cadherin Diffusion in Supported Lipid 570 Bilayers Exhibits Calcium-Dependent Dynamic Heterogeneity". en. In: Biophysical Journal 111.12 (2016), pp. 2658–2665. ISSN: 0006-3495. DOI: 10.1016/j.bpj. 2016.10.037.
 - Susanne F. Fenz et al. "Membrane fluctuations mediate lateral interaction between cadherin bonds". en. In: Nature Physics 13.9 (2017), pp. 906–913. ISSN: 1745-2473, 1745-2481. DOI: 10.1038/nphys4138.
 - B. Ladoux et al. "The mechanotransduction machinery at work at adherens junctions". In: *Integrative Biology* 7.10 (2015), pp. 1109-1119. issn: 1757-9708. doi: 10.1039/ c5ib00070j.
 - Suzie Verma et al. "Arp2/3 activity is necessary for efficient formation of E-cadherin adhesive contacts". en. In: J. Biol. Chem. 279.32 (2004), pp. 34062–34070.
 - Nadia Efimova and Tatyana M. Svitkina. "Branched actin networks push against each other at adherens junctions to maintain cell-cell adhesion". In: Journal of Cell Biology 217.5 (2018), pp. 1827–1845. ISSN: 0021-9525. DOI: 10.1083/jcb.201708103.
 - Yinghao Wu, Barry Honig, and Avinoam Ben-Shaul. "Theory and Simulations of Adhesion Receptor Dimerization on Membrane Surfaces". In: Biophysical Journal 104.6 (2013), pp. 1221–1229. issn: 0006-3495. doi: 10.1016/j.bpj.2013.02.009.
 - Rashmi Priya et al. "ROCK1 but not ROCK2 contributes to RhoA signaling and NMIIA-mediated contractility at the epithelial zonula adherens". en. In: Molecular Biology of the Cell 28.1 (2017). Ed. by Jeffrey D. Hardin, pp. 12-20. ISSN: 1059-1524, 1939-4586. DOI: 10.1091/mbc. e16-04-0262.

- phatidylcholine and phosphatidylethanolamine metabolism 654 in health and disease". en. In: Biochimica et Biophysica 655 604 Acta (BBA) - Biomembranes. Membrane Lipid Therapy: 605 Drugs Targeting Biomembranes 1859.9, Part B (2017), 606 pp. 1558–1572. issn: 0005-2736. doi: 10 . 1016 / j . $_{\tiny 658}$ 607 bbamem. 2017.04.006. (Visited on 05/16/2022). 608
- Bhushan Nagar et al. "Structural basis of calcium-induced 609 42. E-cadherin rigidification and dimerization". en. In: Nature 610 380.6572 (1996), pp. 360–364. ISSN: 1476-4687. DOI: 611 10.1038/380360a0. 612
- 613 43. Lawrence Shapiro and William I. Weis. "Structure and Biochemistry of Cadherins and Catenins". en. In: Cold 614 Spring Harbor Perspectives in Biology 1.3 (2009), a003053. 615 ISSN:, 1943-0264. DOI: 10.1101/cshperspect.a003053
- 44. Otger Campàs et al. "Quantifying cell-generated me- 668 chanical forces within living embryonic tissues". In: Nat. 618 Methods 11.3 (2014), pp. 349-349.
- 45. Michelle R. Emond and James D. Jontes. "Bead Ag- 671 620 gregation Assays for the Characterization of Putative 672 621 Cell Adhesion Molecules". In: Journal of Visualized 673 622 Experiments: JoVE 92 (2014). ISSN: 1940-087X. DOI: 623 10.3791/51762.
- Clair R. Seager and Thomas G. Mason. "Slippery diffusion- 676 625 limited aggregation". en. In: Physical Review E 75.1 677 626 (2007), p. 011406. ISSN: 1539-3755, 1550-2376. DOI: 627 10.1103/PhysRevE.75.011406.
- Jasna Brujić et al. "3D bulk measurements of the force dis-680 tribution in a compressed emulsion system". en. In: Fara-630 day Discussions 123.0 (2003). Publisher: Royal Society of Chemistry, pp. 207–220. DOI: 10.1039/B204414E. 632
- L.-L. Pontani et al. "Biomimetic emulsions reveal the 684 633 effect of mechanical forces on cell-cell adhesion". en. In: 685 Proceedings of the National Academy of Sciences 109.25 635 (2012), pp. 9839-9844. issn: 0027-8424, 1091-6490. 636 DOI: 10.1073/pnas.1201499109. URL: http://www. 637 pnas.org/cgi/doi/10.1073/pnas.1201499109 638 (visited on 02/08/2022).
- 640 49. Yinghao Wu et al. "Transforming binding affinities from three dimensions to two with application to cadherin 641 clustering". en. In: *Nature* 475.7357 (2011), pp. 510–513. 642 ISSN: 0028-0836, 1476-4687. DOI: 10.1038/nature10183. 643
- 644 50. Sam Meyer et al. "Jamming in two-dimensional packings" en. In: Physica A: Statistical Mechanics and its Appli-645 cations 389.22 (2010), pp. 5137-5144. ISSN: 03784371. 646 DOI: 10.1016/j.physa.2010.07.030.
- Pierre-Olivier Strale et al. "The formation of ordered 648 51. nanoclusters controls cadherin anchoring to actin and 649 cell-cell contact fluidity". en. In: J Cell Biol 210.2 650 (2015), pp. 333–346. ISSN: 0021-9525, 1540-8140. DOI: 651 10.1083/jcb.201410111.

- 602 41. Jelske N. van der Veen et al. "The critical role of phos- 653 52. H M Princen. "Rheology of Foams and Highly Concentrated Emulsions". en. In: Journal of Colloid and Interface Science 91.1 (1983), p. 16.
 - 656 53. K. A. Newhall et al. "Size-Topology Relations in Packings of Grains, Emulsions, Foams, and Biological Cells". In: Physical Review Letters 108.26 (2012), p. 268001. DOI: 10.1103/PhysRevLett.108.268001.
 - 54. Ivane Jorjadze, Lea-Laetitia Pontani, and Jasna Brujic. "Microscopic Approach to the Nonlinear Elasticity of Compressed Emulsions". en. In: Physical Review Letters 110.4 (2013), p. 048302. ISSN: 0031-9007, 1079-7114. DOI: 10.1103/PhysRevLett.110.048302.
 - 665 55. Lea-Laetitia Pontani et al. "Immiscible lipids control the morphology of patchy emulsions". en. In: Soft Matter 9.29 (2013), p. 7150. ISSN: 1744-683X, 1744-6848. DOI: 10.1039/c3sm51137e.
 - 56. Connor J Thompson et al. "Cadherin clusters stabilized by a combination of specific and nonspecific cisinteractions". In: eLife 9 (2020). Ed. by Nir Ben-Tal and Olga Boudker, e59035. ISSN: 2050-084X. DOI: 10.7554/ eLife.59035.
 - 674 57. Fei Wu et al. "Homophilic interaction and deformation of E-cadherin and cadherin 7 probed by single molecule force spectroscopy". en. In: Arch. Biochem. Biophys. 587 (2015), pp. 38-47.
 - 678 58. Amy Wang, Alexander R Dunn, and William I Weis. "Mechanism of the cadherin-catenin F-actin catch bond interaction". en. In: Elife 11 (2022).
 - 681 59. Oliver J. Harrison et al. "Two-step adhesive binding by classical cadherins". en. In: Nature Structural & Molecular Biology 17.3 (2010). Number: 3 Publisher: Nature Publishing Group, pp. 348–357. ISSN: 1545-9985. DOI: 10.1038/nsmb.1784.
 - 686 60. Soonjin Hong, Regina B Troyanovsky, and Sergey M Troyanovsky, "Cadherin exits the junction by switching its adhesive bond". en. In: J. Cell Biol. 192.6 (2011), pp. 1073-1083.
 - 690 61. Ramesh Koirala et al. "Inside-out regulation of E-cadherin conformation and adhesion". en. In: Proc. Natl. Acad. Sci. U. S. A. 118.30 (2021), e2104090118.

SUPPLEMENTARY MATERIAL

694 An online supplement to this article can be found by visiting 695 BJ Online at http://www.biophysj.org.